

A Weakly Supervised Transformer to Support Rare Disease Diagnosis from Electronic Health Records: Methods and Applications in Rare Pulmonary Disease

Kimberly F. Greco^{*1}, Zongxin Yang^{*2}, Mengyan Li³, Han Tong⁴, Sara Morini Sweet², Alon Geva^{5,6, 7}, Kenneth D. Mandl^{7,8}, Benjamin A. Raby^{9,10}, and Tianxi Cai^{1,2}

¹Department of Biostatistics, Harvard T.H. Chan School of Public Health, Boston, USA

²Department of Biomedical Informatics, Harvard Medical School, Boston, USA

³Department of Mathematical Sciences, Bentley University, Waltham, USA

⁴Department of Biostatistics, Columbia University, New York, USA

⁵Department of Anesthesiology, Critical Care, and Pain Medicine, Boston Children's Hospital, Boston, USA

⁶Department of Anesthesia, Harvard Medical School, Boston, USA

⁷Computational Health Informatics Program, Boston Children's Hospital, Boston, USA

⁸Department of Pediatrics, Harvard Medical School, Boston, USA

⁹Division of Pulmonary Medicine, Boston's Children Hospital, Harvard Medical School, Boston, USA

¹⁰Channing Division of Network Medicine, Brigham and Women's Hospital, Harvard Medical School, Boston, USA

Abstract

Rare diseases affect an estimated 300-400 million people worldwide, yet individual conditions often remain poorly characterized and difficult to diagnose due to their low prevalence and limited clinician familiarity. While computational phenotyping algorithms show promise for automating rare disease detection, their development is hindered by the scarcity of labeled data and biases in existing label sources. Gold-standard labels from registries and expert chart reviews are highly accurate but constrained by selection bias and the cost of manual review. In contrast, labels derived from electronic health records (EHRs) cover a broader range of patients but can introduce substantial noise. To address these challenges, we propose a weakly supervised, transformer-based framework that combines a small set of gold-standard labels with a large volume of iteratively updated silver-standard labels derived from EHR data. This hybrid approach enables the training of a highly accurate and generalizable phenotyping model that scales rare disease detection beyond the scope of individual clinical expertise. Our method is initialized by learning embeddings of medical concepts based on their semantic meaning or co-occurrence patterns in EHRs, which are then refined and aggregated into patient-level representations via a multi-layer transformer architecture. Using two rare pulmonary diseases as a case study, we validate our model on EHR data from Boston Children's Hospital. Our framework demonstrates notable improvements in phenotype classification, identification of clinically meaningful subphenotypes through patient clustering, and prediction of disease progression compared to baseline methods. These results highlight the potential of our approach to enable scalable identification and stratification of rare disease patients for clinical care and research applications.

^{*}These authors contributed equally to this work.

1. Introduction

Rare diseases are broadly defined as conditions affecting fewer than 1 in 2,000 people in any World Health Organization region or, in the United States, as those affecting fewer than 200,000 people [20, 44]. While individually uncommon, rare diseases collectively impose a significant public health burden, affecting an estimated 300-400 million people worldwide [20, 31]. Among these, approximately 30 million people in the United States – 10% of Americans – are living with a rare disease, a prevalence comparable to that of type 2 diabetes [31, 5].

Despite their widespread impact, rare diseases – spanning more than 7,000 distinct conditions – remain disproportionately difficult to diagnose. Clinicians may encounter some of these conditions only once, if ever, in their careers, limiting their familiarity with the full spectrum of clinical presentations [30, 35]. These challenges contribute to the phenomenon of the “diagnostic odyssey” – a years-long journey marked by inconclusive tests, repeated specialist referrals, and frequent misdiagnoses – experienced by most rare disease patients [4]. On average, these patients consult between three and ten different physicians, with delays ranging from four to seven years before receiving a correct diagnosis [40, 20, 30]. Prolonged diagnostic delays leave patients without effective treatment for extended periods, increasing the risk of preventable complications, disease progression, and premature mortality [39, 18, 32]. This burden is particularly acute in pediatric populations, as 70% of rare diseases have childhood onset, and 30% of affected children die before the age of five – underscoring the urgent need for earlier and more accurate diagnosis to improve pediatric outcomes and support sustained health and quality of life across the lifespan [11, 20].

The challenges of rare disease diagnosis are further magnified in the context of rare pulmonary diseases, which remain notoriously difficult to identify due to their symptomatic overlap with more common respiratory conditions. Up to one-third of individuals initially diagnosed with asthma are later found to have been misdiagnosed, with their symptoms more accurately attributed to less prevalent comorbid conditions [16, 24]. Pulmonary hypertension (PH), a progressive disorder characterized by high blood pressure in the pulmonary arteries, frequently presents with nonspecific symptoms such as breathlessness, fatigue, and weakness – clinical features that closely resemble those of asthma [36, 13]. This overlap often leads to delayed diagnosis, by which point irreversible vascular damage may already be present [6]. Severe asthma, a distinct and high-burden condition requiring treatment with high-dose inhaled corticosteroids plus a second controller, presents a similarly complex diagnostic challenge [9]. Despite accounting for more than one-third of asthma-related deaths, severe asthma remains under-recognized, and its clinical heterogeneity further complicates both timely diagnosis and effective management [26]. Together, these diagnostic pitfalls highlight the limitations of relying solely on clinical expertise and underscore the need for data-driven approaches that can detect subtle, multi-dimensional patterns often missed in routine practice.

Efforts to compile rare disease cases into condition-specific registries have helped consolidate data for research [10], but these registries are typically too small and narrow in scope to support comprehensive rare disease studies [17, 19]. Furthermore, because registry inclusion requires a confirmed diagnosis, individuals with atypical presentations or missed diagnoses – who are critical to building more representative datasets for research – are systematically excluded. The widespread adoption of electronic health records (EHRs) has enabled large-scale investigation of rare diseases across diverse patient populations and care settings, capturing a broader spectrum of clinical presentations than traditional registries. EHRs contain rich longitudinal data in both structured (e.g., diagnosis, medication, and procedure codes) and unstructured (e.g., free-text clinical notes from which we extract concept unique identifiers [CUIs]) formats, collectively documenting a patient’s diagnostic journey – including the misdiagnoses and testing patterns that can help characterize rare diseases [14]. With access to these data, machine-assisted diagnostic

approaches are becoming increasingly integrated into both clinical care and research workflows, with notable success in pulmonary medicine, where they support real-time interpretation of imaging studies [43, 22], flag high-risk individuals for specialist referrals [23], and retrospectively identify undiagnosed patients for inclusion in disease registries and observational studies [15].

Central to these efforts is computational phenotyping, which aims to automate the identification of patterns in EHR data that distinguish patients with a given disease (phenotyping) and further stratify them based on clinically meaningful subgroups such as prognosis or treatment response (subphenotyping). Traditionally, phenotyping has relied on rule-based algorithms that apply predefined logical criteria – such as the presence of a specific diagnostic code or concept, use of a relevant medication, or an abnormal lab value – to infer disease status from a patient’s clinical profile [38, 1]. While effective for well-characterized diseases with standardized coding practices, these methods translate poorly to rare diseases, which are often clinically heterogeneous and lack codified diagnostic criteria [49, 2].

To overcome the limitations of rule-based approaches, machine learning (ML) and, in particular, deep learning (DL) have emerged as powerful alternatives to enable phenotyping at scale [49, 7]. A key innovation in this space is representation learning, which transforms high-dimensional clinical data into lower-dimensional vector spaces that preserve semantic and contextual relationships [8]. Within this framework, medical concepts from both structured and unstructured EHR data are mapped to embeddings pre-trained on co-occurrence patterns and semantic context [45]. These concept-level embeddings can be further aggregated into patient-level representations that support downstream phenotyping and subphenotyping tasks [12].

Despite their success in modeling common diseases, current ML and DL approaches often fail to generalize to rare disease settings. This is due to challenges inherent to both the data and the modeling paradigm. First, EHR data are high-dimensional, sparse, and noisy [3, 37]. Crucially, the presence of a diagnostic code or concept in the EHR does not always indicate a confirmed physician diagnosis – it may be entered for billing purposes, reflect rule-out or provisional conditions, or persist from outdated assessments [48, 46]. Documentation practices vary widely across providers and institutions, further compounding label inconsistency. These factors degrade the reliability of EHR-derived labels and introduce substantial noise into downstream phenotyping tasks. Second, the dominant ML/DL paradigm for phenotyping is supervised learning, which depends on large volumes of high-quality labeled data – a resource rarely available in rare disease contexts. Supervised models often overfit small, gold-standard cohorts and struggle to generalize to broader, more diverse patient populations. As a result, their clinical utility remains limited. These constraints have fueled growing interest in weakly supervised learning, an approach that leverages large quantities of noisy or partially labeled data to improve model performance in low-label settings.

Among emerging deep learning architectures, transformers have shown particular promise for EHR-based phenotyping due to their ability to model complex temporal dependencies and long-range relationships across irregular clinical events [42, 50]. Recent models such as BEHRT [28], Med-BERT [34], RatchetEHR [21], and Foresight [25] have demonstrated impressive performance on a variety of predictive and classification tasks across both structured and unstructured clinical data. These advances underscore the potential of transformer-based models to capture nuanced disease patterns and support scalable phenotyping. However, despite their promise, transformer models remain largely constrained by the same supervised learning paradigm that limits broader ML/DL applications in rare disease settings. Most existing transformer-based approaches depend heavily on large volumes of clean, labeled training data. As a result, their applicability to low-label, high-noise scenarios remains limited, and their potential for rare disease detection is yet to be fully realized.

To address this gap, we propose a weakly supervised transformer framework for rare disease phenotyping and subphenotyping. Our method combines a small set of expert-validated gold-standard labels with a much larger set of iteratively refined silver-standard labels derived from real-world EHR data. By integrating precise supervision with abundant but noisy signals, the model learns robust patient representations optimized for downstream tasks such as classification and clustering. Using PH and severe asthma as motivating case studies, we demonstrate that our approach improves phenotype detection and enables clinically meaningful subgroup discovery in real-world, data-limited settings.

2. Methods

Our end-to-end pipeline integrates representation learning with weak supervision and iterative label refinement to enable accurate and scalable EHR phenotyping. We first identify a high-risk patient cohort and assign initial phenotypic labels using gold- or silver-standard sources (§2.1). Each patient’s longitudinal clinical history is then transformed into a structured input sequence through a multi-step preprocessing pipeline that includes event aggregation, feature selection, and frequency encoding (§2.2). These inputs are processed by a multi-layer transformer encoder that models dependencies among clinical concepts (§2.3). We then aggregate concept-level embeddings to generate patient-level representations, apply a classification head, and iteratively refine the silver-standard labels through weak supervision (§2.4). The framework outputs both a patient-level phenotype prediction and a low-dimensional embedding suitable for clustering and visualization. An overview of the pipeline is shown in Figure 1.

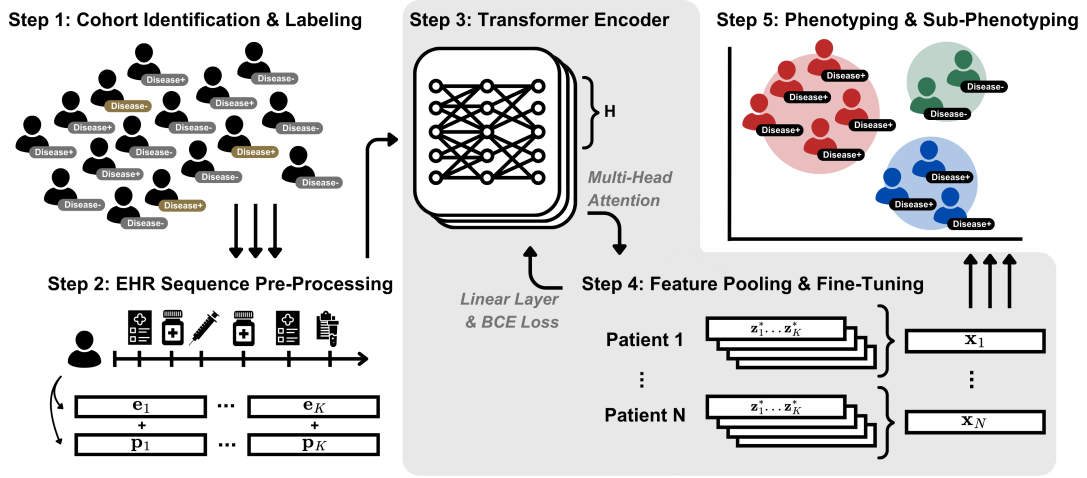


Figure 1: Overview of the proposed weakly supervised transformer framework for EHR-based phenotyping.

2.1. Cohort Identification and Labeling

We start by constructing a high-risk patient cohort – individuals whose EHRs exhibit clinical features suggestive of the target condition or related conditions associated with elevated risk. For each disease-specific task, we designate a target diagnostic code or concept c^* , which serves as an anchor for identifying relevant features and guiding the label refinement process.

Let $i = 1, \dots, N$ index all patients in the high-risk cohort. Each patient i is assigned a label y_i reflecting their phenotype status. Based on the source and reliability of the label, patients are stratified into one of two subcohorts:

1. *Gold-Standard Cohort*: Patients whose disease status has been confirmed through expert physician chart review or inclusion in a dedicated disease registry. These patients are assigned gold-standard labels, denoted y_i^{gold} , which serve as high-fidelity references for model training and evaluation.
2. *Silver-Standard Cohort*: Patients with possible but unconfirmed diagnoses. These patients are assigned silver-standard labels, denoted y_i^{silver} , inferred from the EHR data. Silver-standard labels can be defined using rule-based heuristics – such as exceeding a threshold number of occurrences of c^* – or derived from the probabilistic predictions of automated phenotyping algorithms such as PheNorm [53] or KOMAP [47]. While these criteria expand the size of the labeled dataset, silver-standard labels are inherently noisier and require iterative refinement.

The full set of training labels $\{y_i\}$ is drawn from both cohorts and defined as:

$$y_i = \begin{cases} y_i^{\text{gold}}, & \text{if patient } i \text{ is in the gold-standard cohort,} \\ y_i^{\text{silver}}, & \text{if patient } i \text{ is in the silver-standard cohort.} \end{cases}$$

A central component of our framework is the iterative refinement of silver-standard labels. Unlike gold-standard labels, which remain fixed, silver-standard labels are dynamically updated during model training. After each training round, the model generates updated predictions for the silver-standard cohort, and these predicted probabilities replace the previous labels. This weakly supervised approach allows the model to progressively improve label quality, enabling more accurate phenotype classification while leveraging the scale and diversity of real-world EHR data.

2.2. EHR Sequence Pre-Processing

We transform each patient’s raw EHR into a structured representation suitable for transformer-based learning. This pre-processing pipeline comprises three key stages: (1) sequential representation of clinical histories, (2) label-aware augmentation for gold-standard patients, and (3) construction of input embeddings via feature selection and frequency encoding.

2.2.1 Sequential Representation of EHR Data

For each patient i , the EHR is modeled as a temporal sequence of clinical events partitioned into discrete time windows. These windows reflect clinically meaningful periods such as visits, months, or hospitalization episodes. Let the patient sequence be:

$$\mathcal{P} = \{\mathcal{V}_1, \mathcal{V}_2, \dots, \mathcal{V}_T\},$$

where T is the number of observed time windows. Each window \mathcal{V}_t contains a set of documented medical concepts and their associated occurrence counts:

$$\mathcal{V}_t = \{(c_{t1}, n_{t1}), (c_{t2}, n_{t2}), \dots, (c_{tK_t}, n_{tK_t})\},$$

where c_{tk} denotes a medical concept and n_{tk} the number of times it was recorded in window \mathcal{V}_t . The number of concepts K_t may vary across windows and patients.

2.2.2 Label-Aware Augmentation for Gold-Standard Patients

To enhance generalization and enable effective learning from high-quality labeled examples, we apply two augmentation strategies to the gold-standard cohort: oversampling and dynamic temporal truncation. These methods address class imbalance between gold- and silver-standard cohorts and introduce variability into training.

First, we mitigate the limited size of the gold-standard cohort by oversampling. Each gold-standard patient is replicated r times in the training data, ensuring that high-confidence examples are adequately represented and not overshadowed by the larger, noisier silver cohort. This increases the frequency with which the model encounters trusted labels during training, reinforcing supervision from reliable examples.

Second, we apply temporal truncation to simulate the incompleteness and variability typical of real-world EHRs. During each training iteration, for a patient sequence $\mathcal{P} = \{\mathcal{V}_1, \dots, \mathcal{V}_T\}$, we randomly sample a start and end index, t_{start} and t_{end} , such that $1 \leq t_{\text{start}} \leq t_{\text{end}} \leq T$. The truncated sequence is defined as:

$$\mathcal{P}' = \{\mathcal{V}_{t_{\text{start}}}, \dots, \mathcal{V}_{t_{\text{end}}}\}.$$

This exposes the model to a variety of partial clinical trajectories – some early, some late – mimicking patients presenting at different disease stages or lacking complete documentation. Over time, this dynamic sampling increases the diversity of training examples derived from a fixed gold-standard set and improves robustness to temporal variability in real-world EHR data.

2.2.3 Feature Engineering and Embedding Construction

To prepare each sequence \mathcal{P} or its truncated version \mathcal{P}' as input to the transformer, we construct a structured representation through several pre-processing steps.

(a) Concept Aggregation and Pre-Trained Embeddings

Let $\mathcal{C} = \{(c_1, n_1), (c_2, n_2), \dots, (c_K, n_K)\}$ denote the set of unique concepts and their cumulative counts across a patient’s selected time period, whether from \mathcal{P} or \mathcal{P}' . Each concept $c_k \in \mathcal{C}$ is mapped to a vector representation \mathbf{e}_k using a pre-trained embedding model (PEM) such as SapBERT [29], CODER [54], MUGS [27], or ONCE [47]:

$$\mathbf{e}_k = \text{PEM}(c_k), \quad \mathbf{e}_k \in \mathbb{R}^{d_{\text{input}}}. \quad (1)$$

Since the transformer model operates in a hidden space of dimension d_{model} , we project each embedding into this space via a learnable linear transformation:

$$\mathbf{e}_k^{\text{proj}} = \mathbf{W}^{\text{proj}} \mathbf{e}_k + \mathbf{b}^{\text{proj}}, \quad \mathbf{e}_k^{\text{proj}} \in \mathbb{R}^{d_{\text{model}}}, \quad (2)$$

where $\mathbf{W}^{\text{proj}} \in \mathbb{R}^{d_{\text{model}} \times d_{\text{input}}}$ and $\mathbf{b}^{\text{proj}} \in \mathbb{R}^{d_{\text{model}}}$ are learnable parameters.

(b) Similarity-Based Feature Selection

Given the potentially large number of unique concepts in \mathcal{C} , we perform feature selection to retain only those most relevant to the target condition. This serves two purposes: (1) reducing noise from unrelated concepts, and (2) lowering computational burden, since transformer attention scales quadratically with the number of input tokens.

To identify relevant features, we compute the cosine similarity between the embedding of each concept and that of the target concept c^* for each patient:

$$S(c_k, c^*) = \frac{\mathbf{e}_k \cdot \mathbf{e}^*}{\|\mathbf{e}_k\| \|\mathbf{e}^*\|}, \quad (3)$$

where \mathbf{e}_k and \mathbf{e}^* are the respective embeddings. The top K^* concepts with the highest similarity scores are retained:

$$\mathcal{C}^* = \{(c_1, n_1), (c_2, n_2), \dots, (c_{K^*}, n_{K^*})\}, \quad \text{where } S(c_1, c^*) \geq S(c_2, c^*) \geq \dots \geq S(c_{K^*}, c^*).$$

The target c^* is always included to ensure phenotype-specific information is preserved. Each n_k denotes the total count of concept c_k across all relevant time windows.

(c) Concept Frequency Encoding

At this stage, we have constructed an aggregated set \mathcal{C}^* comprising unique clinical concepts and their corresponding cumulative frequencies, which summarize a patient’s longitudinal medical history. To encode concept frequency – used here as a proxy for clinical significance, capturing aspects such as chronicity or ongoing management – we introduce a frequency-based embedding mechanism.

Each cumulative count n_k for concept c_k is projected into the model’s embedding space through a two-layer feedforward network with a SwiGLU activation function:

$$\mathbf{p}_k = \mathbf{W}_2^{\text{pos}} \text{SwiGLU}(n_k \mathbf{W}_1^{\text{pos}} + \mathbf{b}_1^{\text{pos}}) + \mathbf{b}_2^{\text{pos}}, \quad \mathbf{p}_k \in \mathbb{R}^{d_{\text{model}}}, \quad (4)$$

with learnable parameters:

$$\mathbf{W}_1^{\text{pos}} \in \mathbb{R}^{\frac{d_{\text{model}}}{2} \times 1}, \quad \mathbf{W}_2^{\text{pos}} \in \mathbb{R}^{d_{\text{model}} \times \frac{d_{\text{model}}}{2}}, \quad \mathbf{b}_1^{\text{pos}} \in \mathbb{R}^{\frac{d_{\text{model}}}{2}}, \quad \mathbf{b}_2^{\text{pos}} \in \mathbb{R}^{d_{\text{model}}}.$$

Unlike traditional positional encodings used in NLP, this representation is grounded in concept frequency rather than token order, offering a tailored signal for clinical models sensitive to the recurrence and persistence of medical events.

(d) Transformer Input Sequence

The final representation of each selected concept is obtained by summing its embedding and frequency encoding:

$$\mathbf{z}_k = \mathbf{e}_k^{\text{proj}} + \mathbf{p}_k, \quad \mathbf{z}_k \in \mathbb{R}^{d_{\text{model}}}. \quad (5)$$

Here, \mathbf{z}_k is the input token for concept c_k to the transformer. This formulation allows the model to simultaneously capture semantic similarity across medical concepts and their implicit clinical significance based on frequency. The final patient sequence is:

$$\mathbf{Z}_i = \{\mathbf{z}_1, \mathbf{z}_2, \dots, \mathbf{z}_{K^*}\}.$$

2.3. Transformer Encoder

The model is a multi-layer transformer-based architecture that serves dual purposes: weakly supervised patient classification and representation learning for unsupervised clustering. It processes sequences of medical concepts derived from patient EHRs and models complex dependencies using stacked transformer encoder layers. Through this architecture, the model produces a probability score for phenotype prediction and simultaneously generates a low-dimensional patient embedding that can be used for downstream tasks such as clustering, subtyping, or visualization.

2.3.1 Multi-Head Attention

Each transformer encoder layer applies multi-head self-attention to capture interactions between medical concepts. Given input embeddings $\mathbf{z}_k \in \mathbf{Z}_i$, the model computes queries, keys, and values using learnable projection matrices $\mathbf{W}_Q, \mathbf{W}_K, \mathbf{W}_V \in \mathbb{R}^{d_{\text{model}} \times d_{\text{model}}}$. The self-attention mechanism is split into H heads, each operating in a subspace of dimension $d_h = \frac{d_{\text{model}}}{H}$. For each head $h \in \{1, \dots, H\}$, input embeddings are projected as:

$$\mathbf{q}_k^{(h)} = \mathbf{W}_Q^{(h)} \mathbf{z}_k, \quad \mathbf{k}_k^{(h)} = \mathbf{W}_K^{(h)} \mathbf{z}_k, \quad \mathbf{v}_k^{(h)} = \mathbf{W}_V^{(h)} \mathbf{e}_k^{\text{proj}}, \quad (6)$$

This multi-head design enables the model to attend to diverse contextual patterns across the input sequence. Attention weights within each head are computed using scaled dot-product attention:

$$\text{score}_{kj}^{(h)} = \frac{\mathbf{q}_k^{(h)} \cdot \mathbf{k}_j^{(h)}}{\sqrt{d_h}}, \quad (7)$$

followed by normalization with the softmax function:

$$\alpha_{kj}^{(h)} = \text{softmax}(\text{score}_{kj}^{(h)}), \quad (8)$$

which determines the influence of concept j on concept k . The attention-based output for each head is:

$$\mathbf{z}_k^{(h)} = \sum_j \alpha_{kj}^{(h)} \mathbf{v}_j^{(h)}. \quad (9)$$

2.3.2 Concatenation and Linear Projection

Outputs from all attention heads are concatenated to restore the full embedding dimension:

$$\mathbf{z}_k^{\text{attn}} = \text{Concat}(\mathbf{z}_k^{(1)}, \dots, \mathbf{z}_k^{(H)}), \quad \mathbf{z}_k^{\text{attn}} \in \mathbb{R}^{d_{\text{model}}}. \quad (10)$$

A final linear projection aggregates information across heads:

$$\mathbf{z}_k^{\text{out}} = \mathbf{W}^{\text{out}} \mathbf{z}_k^{\text{attn}}, \quad (11)$$

where $\mathbf{W}^{\text{out}} \in \mathbb{R}^{d_{\text{model}} \times d_{\text{model}}}$ is a learnable weight matrix. To promote stable training and gradient flow, we apply a residual connection followed by layer normalization:

$$\mathbf{z}_k^{\text{norm}} = \text{LayerNorm}(\mathbf{z}_k + \text{Dropout}(\mathbf{z}_k^{\text{out}})). \quad (12)$$

2.3.3 Feedforward Network with SwiGLU Activation

Each transformer layer includes a position-wise feedforward network with two linear layers and a SwiGLU activation:

$$\mathbf{z}_k^{\text{ffn}} = \mathbf{W}_2^{\text{ffn}} \text{SwiGLU}(\mathbf{W}_1^{\text{ffn}} \mathbf{z}_k^{\text{norm}} + \mathbf{b}_1^{\text{ffn}}) + \mathbf{b}_2^{\text{ffn}}. \quad (13)$$

A second residual connection and layer normalization step complete the transformer block:

$$\mathbf{z}_k^* = \text{LayerNorm}(\mathbf{z}_k^{\text{norm}} + \text{Dropout}(\mathbf{z}_k^{\text{ffn}})). \quad (14)$$

2.4. Feature Pooling and Fine Tuning

After passing through multiple transformer layers, the sequence of contextualized embeddings is aggregated into a fixed-length patient representation using mean pooling:

$$\mathbf{x}_i = \frac{1}{K^*} \sum_{k=1}^{K^*} \mathbf{z}_k^*. \quad (15)$$

This approach allows the model to capture contributions from all medical concepts while accommodating sequences of varying lengths. The pooled patient representation \mathbf{x}_i is passed through a classification head – a linear layer followed by a sigmoid activation – to produce a probability score:

$$p(y_i) = \sigma(\mathbf{W}^{\text{class}} \mathbf{x}_i + \mathbf{b}^{\text{class}}), \quad (16)$$

where $\mathbf{W}^{\text{class}}$ and $\mathbf{b}^{\text{class}}$ are learnable parameters. The sigmoid function $\sigma(\cdot)$ maps the logit to a probability in the range $[0, 1]$. Model training uses binary cross-entropy (BCE) loss:

$$\mathcal{L}_{\text{BCE}} = -\frac{1}{N} \sum_{i=1}^N [y_i \log(p(y_i)) + (1 - y_i) \log(1 - p(y_i))], \quad (17)$$

which penalizes confident but incorrect predictions and encourages well-calibrated outputs. After each training round, the best-performing model on the validation set is used to update silver-standard labels using its predicted probabilities:

$$y_i^{\text{silver}} \leftarrow p(y_i). \quad (18)$$

This iterative label refinement allows the model to incorporate its own predictions, progressively improving phenotype classification over training cycles.

3. Results

We evaluated our framework on two rare pulmonary diseases: PH and severe asthma. For each disease, the model was trained and validated independently using disease-specific cohorts and labels curated from EHR data at BCH.

3.1. Data Curation

For both PH and severe asthma, we constructed disease-specific cohorts by first identifying an at-risk patient population. The at-risk PH cohort was defined as patients with PheCode 415.2 (suggestive of potential PH), while the severe asthma cohort included patients with PheCodes beginning with J45 (suggestive of asthma of any severity).

The gold-standard cohorts consisted of patients with a confirmed diagnosis, either through expert chart review or enrollment in a disease-specific registry. These high-fidelity labels (y_i^{gold}) were used for model evaluation and to calibrate the probabilistic silver-standard labels. The PH gold-standard cohort included 531 patients, and the severe asthma cohort included 248 patients. Each cohort was randomly split into 80% training and 20% test sets, with the test set further divided into two cross-validation folds.

The silver-standard cohorts consisted of the remaining at-risk patients whose phenotype status was not definitively adjudicated – 13,774 for PH and 7,387 for severe asthma. To assign initial probabilistic labels ($y_i^{\text{silver}} \in [0, 1]$) to these patients, we applied the KOMAP algorithm, an unsupervised phenotyping approach that generates phenotype likelihood scores from EHR data [47].

For PH, KOMAP was applied to structured, codified EHR data such as diagnosis and procedure codes. For severe asthma, KOMAP incorporated both codified and unstructured clinical data. Natural language features were extracted from clinical notes using two natural language processing (NLP) tools: NILE for named entity recognition [52], and GENIE for relation-aware information extraction [51]. We specifically targeted mentions of PheCode:415.2 for PH and CUI:C0581126 for severe asthma, corresponding to “severe asthma” in free-text notes.

To improve the interpretability and calibration of KOMAP’s unsupervised outputs, we trained a logistic regression model using the gold-standard subset. This calibration procedure involved three steps: (1) subsetting to patients with gold-standard labels, (2) fitting a logistic model to predict y_i^{gold} from the initial KOMAP scores, and (3) applying the fitted model to the full cohort to generate calibrated probabilities. These values were used as the initial silver-standard labels in our weakly supervised learning framework.

For representation learning, we mapped the codified EHR data in the PH cohort to pre-trained MUGS embeddings [27] and the NLP-derived features in the severe asthma cohort to pre-trained ONCE embeddings [47].

3.2. Pulmonary Hypertension

3.2.1 Classification Performance

We evaluated the transformer model using two cross-validation folds, each involving a split of the same 106 gold-standard patients into validation and test subsets. The validation set was used to select the best-performing model checkpoint within each fold, which was then evaluated on an unseen test subset of 53 patients from BCH. Performance metrics – including area under the curve (AUC) and positive predictive value (PPV) – were computed for each fold and averaged.

We compared the transformer’s performance to three baselines: (1) a simple rule-based approach based on counts of PH-related PheCodes, (2) the initial silver-standard probabilities produced by KOMAP, (3) a supervised XGBoost model trained on the same features. As shown in Table 1, the transformer outperformed all baselines across key metrics. With sensitivity fixed at 85% for all methods, the transformer achieved the highest AUC (0.913) and PPV (0.876), indicating stronger discriminative performance and more reliable identification of true positives. These results highlight the transformer’s consistent advantages over both knowledge-driven and machine learning-based baselines for phenotyping patients with PH.

Metric	Count	KOMAP	XGBoost	Transformer
AUC	0.8450	0.858	0.820	0.913
PPV	0.651	0.808	0.855	0.876

Table 1: Phenotype classification performance for pulmonary hypertension. Transformer metrics are averaged across two cross-validation folds.

3.2.2 Clustering Performance

To evaluate whether our learned patient representations capture meaningful clinical heterogeneity, we applied t-distributed stochastic neighbor embedding (t-SNE) to reduce the dimensionality of the embeddings and visualize patient distributions [41]. As shown in Figure 2, PH+ and PH- patients are more distinctly separated in the latent space when using transformer-derived embeddings compared to traditional feature engineering approaches. In particular, we compared against embeddings generated using term frequency-inverse document frequency (TF-IDF), a classical technique that weights clinical codes based on their relative frequency across patients [33]. While TF-IDF captures code importance in a sparse and interpretable manner, it lacks the contextual awareness and representation capacity of transformer-based models. The improved phenotype separation in the transformer space suggests that our model learns more clinically meaningful patient representations.

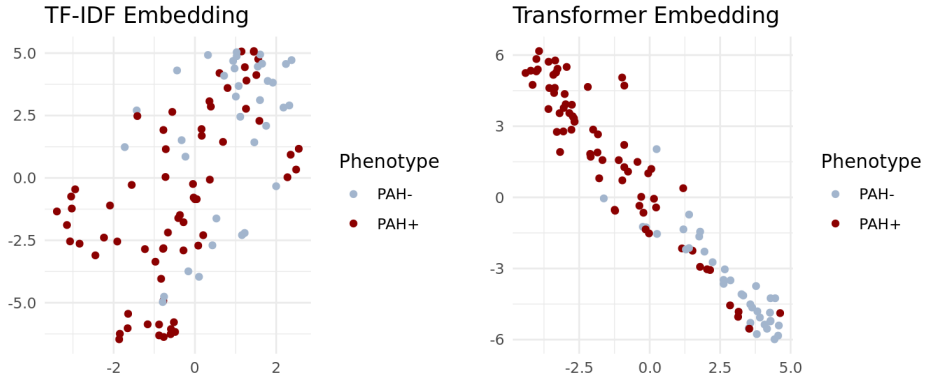


Figure 2: t-SNE visualization of patient-level embeddings shows improved separation of PH+ and PH- phenotypes using transformer-based representations.

To further investigate heterogeneity within the PH+ population, we applied principal component analysis (PCA) to the transformer-derived patient embeddings and retained the top components that collectively explained at least 99% of the variance. We then performed k -means clustering on the reduced embeddings, identifying two distinct subphenotypes. The first group, referred to as the *Slow Progression Cluster* ($n = 53$), consisted of patients with milder

disease trajectories and lower long-term mortality. The second group, labeled the *Fast Progression Cluster* ($n = 16$), included patients with more severe clinical courses and elevated mortality risk. Kaplan–Meier survival analysis revealed a significant difference in 5-year mortality between the two clusters, with the fast progression cluster experiencing markedly worse survival outcomes (log-rank $p = 0.0014$; Figure 3).

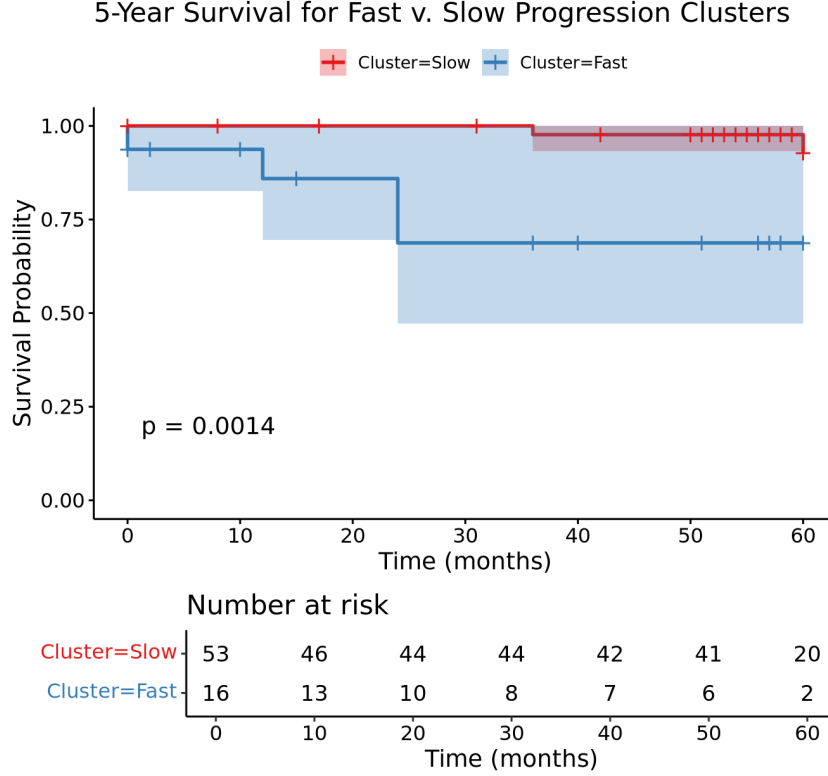


Figure 3: Kaplan-Meier survival curves for PH subgroups identified via k-means clustering of transformer embeddings.

3.3. Severe Asthma

3.3.1 Clustering Performance

To investigate heterogeneity among patients with severe asthma, we applied PCA to the transformer-derived patient embeddings, following a similar approach to the PH analysis. We retained the top components explaining at least 99% of the variance and then applied constrained k-means clustering to the reduced embeddings to identify distinct subphenotypes. We subsequently evaluated the resulting clusters with respect to two high-severity outcomes: recurrent low oxygen episodes (e.g., hypoxia, hypoxemia, oxygen desaturation) and respiratory failure. This analysis revealed two clinically meaningful subgroups: a *Low-Risk Exacerbator Cluster* and a *High-Risk Exacerbator Cluster*. Patients in the high-risk cluster exhibited a 15.1-fold increased hazard of low oxygen events (hazard ratio [HR] = 15.11, 95% confidence interval [CI]: 2.74–83.31, $p = 0.0018$) and a 21.6-fold increased hazard of respiratory failure (HR = 21.56, 95% CI: 2.92–159.2, $p = 0.0026$) compared to those in the low-risk cluster. These findings suggest that the high-risk cluster represents a distinct and more severe asthma trajectory, characterized by frequent respiratory compromise and increased need for acute interventions. This subphenotype may benefit from closer clinical monitoring and more proactive management strategies.

4. Conclusion

This work presents a weakly supervised transformer framework for rare disease phenotyping that addresses two central challenges in this research area: limited access to high-quality labels and the need for robust patient representations in heterogeneous EHR data. By combining a small set of gold-standard labels with a large, diverse cohort annotated through probabilistic silver-standard labels, our approach enables effective learning in real-world, label-scarce settings. We demonstrate that the model not only outperforms existing baselines in phenotype classification, but also learns patient embeddings that support meaningful subphenotype discovery and clinical outcome prediction.

Our method contributes a flexible and generalizable strategy for automated phenotyping, integrating EHR-derived embeddings, dynamic label refinement, and transformer-based representation learning in a unified framework. Through case studies in PH and severe asthma, we demonstrate that the transformer model captures nuanced clinical patterns, stratifies disease progression risk, and facilitates downstream tasks such as survival analysis and clustering.

Future directions include enhancing the interpretability of learned representations to support clinical decision-making, validating model performance across multiple institutions and disease areas, and exploring active learning strategies to efficiently incorporate clinician feedback. By bridging algorithmic innovation with practical clinical utility, our framework moves a step closer to enabling scalable, data-driven diagnosis and risk stratification in rare disease populations.

References

- [1] Hadeel Alzoubi et al. “A review of automatic phenotyping approaches using electronic health records”. In: *Electronics* 8.11 (2019), p. 1235.
- [2] Juan M Banda et al. “Advances in electronic phenotyping: from rule-based definitions to machine learning models”. In: *Annual review of biomedical data science* 1.1 (2018), pp. 53–68.
- [3] Jineta Banerjee et al. “Machine learning in rare disease”. In: *Nature Methods* 20.6 (2023), pp. 803–814.
- [4] Alicia Bauskis et al. “The diagnostic odyssey: insights from parents of children living with an undiagnosed condition”. In: *Orphanet journal of rare diseases* 17.1 (2022), p. 233.
- [5] Vanessa Boulanger et al. “Establishing patient registries for rare diseases: rationale and challenges”. In: *Pharmaceutical Medicine* 34.3 (2020), pp. 185–190.
- [6] Lynette M Brown et al. “Delay in recognition of pulmonary arterial hypertension: factors identified from the REVEAL Registry”. In: *Chest* 140.1 (2011), pp. 19–26.
- [7] Tiffany J Callahan et al. “Characterizing Patient Representations for Computational Phenotyping”. In: *AMIA Annual Symposium Proceedings*. Vol. 2022. 2023, p. 319.
- [8] Edward Choi et al. “Multi-layer representation learning for medical concepts”. In: *proceedings of the 22nd ACM SIGKDD international conference on knowledge discovery and data mining*. 2016, pp. 1495–1504.
- [9] Kian Fan Chung. “Diagnosis and management of severe asthma”. In: *Seminars in Respiratory and Critical Care Medicine*. Vol. 39. 01. Thieme Medical Publishers. 2018, pp. 091–099.
- [10] Hedwig MA D’Agnolo et al. “Creating an effective clinical registry for rare diseases”. In: *United European Gastroenterology Journal* 4.3 (2016), pp. 333–338.

- [11] eClinicalMedicine. “Raising the voice for rare diseases: under the spotlight for equity”. In: *EClinicalMedicine* 57 (2023), p. 101941. DOI: 10.1016/j.eclinm.2023.101941. URL: <https://doi.org/10.1016/j.eclinm.2023.101941>.
- [12] Egill A Fridgeirsson, David Sontag, and Peter Rijnbeek. “Attention-based neural networks for clinical prediction modelling on electronic health records”. In: *BMC medical research methodology* 23.1 (2023), p. 285.
- [13] Nazzareno Galiè et al. “2015 ESC/ERS guidelines for the diagnosis and treatment of pulmonary hypertension: the joint task force for the diagnosis and treatment of pulmonary hypertension of the European Society of Cardiology (ESC) and the European Respiratory Society (ERS): endorsed by: Association for European Paediatric and Congenital Cardiology (AEPC), International Society for Heart and Lung Transplantation (ISHLT)”. In: *European heart journal* 37.1 (2016), pp. 67–119.
- [14] Nicolas Garcelon et al. “Electronic health records for the diagnosis of rare diseases”. In: *Kidney international* 97.4 (2020), pp. 676–686.
- [15] Alon Geva et al. “A computable phenotype improves cohort ascertainment in a pediatric pulmonary hypertension registry”. In: *The Journal of pediatrics* 188 (2017), pp. 224–231.
- [16] Alina Gherasim, Ahn Dao, and Jonathan A Bernstein. “Confounders of severe asthma: diagnoses to consider when asthma symptoms persist despite optimal therapy”. In: *World Allergy Organization Journal* 11 (2018), pp. 1–11.
- [17] RE Gliklich, NA Dreyer, and MB Leavy. *Registries for evaluating patient outcomes: a user’s guide [Internet], 3rd edn. Agency for Healthcare Research and Quality (US), Rockville, MD. Adverse Event Detection, Processing, and Reporting.* 2014.
- [18] Emer Gunne et al. “A retrospective review of the contribution of rare diseases to paediatric mortality in Ireland”. In: *Orphanet Journal of Rare Diseases* 15 (2020), pp. 1–8.
- [19] Isabel C Hageman et al. “A systematic overview of rare disease patient registries: challenges in design, quality management, and maintenance”. In: *Orphanet Journal of Rare Diseases* 18.1 (2023), p. 106.
- [20] The Lancet Global Health. *The landscape for rare diseases in 2024.* 2024.
- [21] Ortal Hirszowicz and Dvir Aran. “ICU Bloodstream Infection Prediction: A Transformer-Based Approach for EHR Analysis”. In: *International Conference on Artificial Intelligence in Medicine.* Springer. 2024, pp. 279–292.
- [22] Peng Huang et al. “Deep machine learning predicts cancer risk in follow-up lung screening”. In: (2019).
- [23] Alan Kaplan et al. “Artificial intelligence/machine learning in respiratory medicine and potential role in asthma and COPD diagnosis”. In: *The Journal of Allergy and Clinical Immunology: In Practice* 9.6 (2021), pp. 2255–2261.
- [24] Joanne Kavanagh, David J Jackson, and Brian D Kent. “Over-and under-diagnosis in asthma”. In: *Breathe* 15.1 (2019), e20–e27.
- [25] Zeljko Kraljevic et al. “Foresight—a generative pretrained transformer for modelling of patient timelines using electronic health records: a retrospective modelling study”. In: *The Lancet Digital Health* 6.4 (2024), e281–e290.
- [26] Mark L Levy et al. *Why asthma still kills: the National Review of Asthma Deaths (NRAD).* 2014.
- [27] Mengyan Li et al. “Multi-Source Graph Synthesis (MUGS) for Pediatric Knowledge Graphs from Electronic Health Records”. In: *medRxiv* (2024), pp. 2024–01.

- [28] Yikuan Li et al. “BEHRT: transformer for electronic health records”. In: *Scientific reports* 10.1 (2020), p. 7155.
- [29] Fangyu Liu et al. “Self-alignment pretraining for biomedical entity representations”. In: *arXiv preprint arXiv:2010.11784* (2020).
- [30] Chloe Miu Mak et al. “Computer-assisted patient identification tool in inborn errors of metabolism—potential for rare disease patient registry and big data analysis”. In: *Clinica Chimica Acta* 561 (2024), p. 119811.
- [31] Shruti Marwaha, Joshua W Knowles, and Euan A Ashley. “A guide for the diagnosis of rare and undiagnosed disease: beyond the exome”. In: *Genome medicine* 14.1 (2022), p. 23.
- [32] Monica Mazzucato et al. “Estimating mortality in rare diseases using a population-based registry, 2002 through 2019”. In: *Orphanet Journal of Rare Diseases* 18.1 (2023), p. 362.
- [33] Juan Ramos et al. “Using tf-idf to determine word relevance in document queries”. In: *Proceedings of the first instructional conference on machine learning*. Vol. 242. 1. Citeseer. 2003, pp. 29–48.
- [34] Laila Rasmy et al. “Med-BERT: pretrained contextualized embeddings on large-scale structured electronic health records for disease prediction”. In: *NPJ digital medicine* 4.1 (2021), p. 86.
- [35] Yaffa R Rubinstein et al. “The case for open science: rare diseases”. In: *JAMIA open* 3.3 (2020), pp. 472–486.
- [36] Nicole F Ruopp and Barbara A Cockrill. “Diagnosis and treatment of pulmonary arterial hypertension: a review”. In: *Jama* 327.14 (2022), pp. 1379–1391.
- [37] Julia Schaefer et al. “The use of machine learning in rare diseases: a scoping review”. In: *Orphanet journal of rare diseases* 15 (2020), pp. 1–10.
- [38] Chaitanya Shivade et al. “A review of approaches to identifying patient phenotype cohorts using electronic health records”. In: *Journal of the American Medical Informatics Association* 21.2 (2014), pp. 221–230.
- [39] Antoine G Sreih et al. “Diagnostic delays in vasculitis and factors associated with time to diagnosis”. In: *Orphanet Journal of Rare Diseases* 16 (2021), pp. 1–8.
- [40] James K Stoller. “The challenge of rare diseases”. In: *Chest* 153.6 (2018), pp. 1309–1314.
- [41] Laurens Van der Maaten and Geoffrey Hinton. “Visualizing data using t-SNE.” In: *Journal of machine learning research* 9.11 (2008).
- [42] A Vaswani. “Attention is all you need”. In: *Advances in Neural Information Processing Systems* (2017).
- [43] Simon LF Walsh et al. “Deep learning for classifying fibrotic lung disease on high-resolution computed tomography: a case-cohort study”. In: *The Lancet Respiratory Medicine* 6.11 (2018), pp. 837–845.
- [44] Chihui Mary Wang et al. “Operational description of rare diseases: a reference to improve the recognition and visibility of rare diseases”. In: *Orphanet Journal of Rare Diseases* 19.1 (2024), p. 334.
- [45] Wei-Hung Weng and Peter Szolovits. “Representation learning for electronic health records”. In: *arXiv preprint arXiv:1909.09248* (2019).
- [46] Hulin Wu et al. *Statistics and machine learning methods for EHR data: From Data Extraction to Data Analytics*. CRC Press, 2020.
- [47] Xin Xiong et al. “Knowledge-driven online multimodal automated phenotyping system”. In: *medRxiv* (2023), pp. 2023–09.

- [48] Jenny Yang et al. “Addressing label noise for electronic health records: insights from computer vision for tabular data”. In: *BMC Medical Informatics and Decision Making* 24.1 (2024), p. 183.
- [49] Siyue Yang et al. “Machine learning approaches for electronic health records phenotyping: a methodical review”. In: *Journal of the American Medical Informatics Association* 30.2 (2023), pp. 367–381.
- [50] Zhichao Yang et al. “TransformEHR: transformer-based encoder-decoder generative model to enhance prediction of disease outcomes using electronic health records”. In: *Nature communications* 14.1 (2023), p. 7857.
- [51] Huaiyuan Ying et al. “GENIE: Generative Note Information Extraction model for structuring EHR data”. In: *arXiv preprint arXiv:2501.18435* (2025).
- [52] Sheng Yu, Tianrun Cai, and Tianxi Cai. “NILE: fast natural language processing for electronic health records”. In: *arXiv preprint arXiv:1311.6063* (2013).
- [53] Sheng Yu et al. “Enabling phenotypic big data with PheNorm”. In: *Journal of the American Medical Informatics Association* 25.1 (2018), pp. 54–60.
- [54] Zheng Yuan et al. “CODER: Knowledge-infused cross-lingual medical term embedding for term normalization”. In: *Journal of biomedical informatics* 126 (2022), p. 103983.